PROCEEDINGS A

rspa.royalsocietypublishing.org

Research

Cite this article: Gordon PV, Gotti DJ, Hegde UG, Hicks MC, Kulis MJ, Sivashinsky GI. 2015 An elementary model for autoignition of laminar jets. *Proc. R. Soc. A* **471**: 20150059. http://dx.doi.org/10.1098/rspa.2015.0059

Received: 28 January 2015
Accepted: 1 June 2015

Subject Areas:
differential equations, mathematical modelling, applied mathematics

Keywords:
autoignition, hydrothermal flames, diffusion flames, heat equation, blow-up, thermal runaway

Author for correspondence:
Peter V. Gordon
e-mail: pgordon@uakron.edu

THE ROYAL SOCIETY PUBLISHING

An elementary model for autoignition of laminar jets

Peter V. Gordon[1], Daniel J. Gotti[2], Uday G. Hegde[4], Michael C. Hicks[3], Michael J. Kulis[3] and Gregory I. Sivashinsky[5]

[1]Department of Mathematics, The University of Akron, Akron, OH 44325, USA
[2]Universities Space Research Association, and [3]NASA Glenn Research Center, Cleveland, OH 44135, USA
[4]Case Western Reserve University, Cleveland, OH 44106, USA
[5]School of Mathematical Sciences, Tel Aviv University, Tel Aviv 69978, Israel

In this paper, we formulate and analyse an elementary model for autoignition of cylindrical laminar jets of fuel injected into an oxidizing ambient at rest. This study is motivated by renewed interest in analysis of hydrothermal flames for which such configuration is common. As a result of our analysis, we obtain a sharp characterization of the autoignition position in terms of the principal physical and geometrical parameters of the problem.

1. Introduction

Autoignition is the process of an abrupt growth of the reaction rate in an explosive system being initially in a non-reactive state. Theoretical studies of autoignition can be traced back to the classical works of Semenov, Frank-Kamentskii and Zeldovich, see [1, 2]. Analysis of autoignition of premixed and non-premixed flames has been performed by many authors in different situations and at different levels of complexity [3–7]. In particular, in the context of non-premixed flames, the ignition studies were predominantly undertaken for a counter-flow configuration [8–10]. In this paper, we propose an elementary model for autoignition of diffusion flames in laminar jets of fuel injected into an oxidizing ambient at rest. To the best of our knowledge, mathematical studies of this configuration have not previously been undertaken. Our analysis of autoignition in this particular configuration is motivated by recent interest in hydrothermal flames for which such a configuration is common.

© 2015 The Author(s) Published by the Royal Society. All rights reserved.

Hydrothermal flames are diffusion flames produced in aqueous environments at conditions above the thermodynamic critical point of water with temperatures and pressures exceeding 374°C and 221 bar, respectively. These flames were first reported in the late 1980s [11] and since then have been studied by many researchers (see [12] for a recent review of experimental results). When conditions are suitable (i.e. temperatures above the ignition temperature with reactant concentrations at appropriate levels), hydrothermal flames can be observed. These conditions are often reached (sometimes unintentionally) during the oxidation reactions taking place in reactors designed to operate above the critical point of water. Due to the renewed interest in supercritical water oxidation (SCWO) as an advantageous technology for the complete and highly efficient destruction of aqueous organic waste streams, recent research has been directed towards understanding the physical processes that cause flames to evolve from the relatively low-temperature oxidation reactions for which most SCWO reactors are designed.

In a typical SCWO reactor, an aqueous waste stream comprising 10–30% of organic waste is introduced at conditions above the critical point of water. Organic compounds and gases (e.g. O_2) readily mix in supercritical water and when temperatures are sufficiently high oxidation reactions take place at very high reaction rates resulting in nearly perfect conversion efficiencies (often above 99.9%) in very brief reactor residence times [12–14]. The SCWO processing of organic waste shows many strong advantages over conventional technologies from both the perspective of efficiency and the perspective of being a 'green technology', owing to the fact that there is often sufficient thermal energy released from the oxidation of the organic waste to allow the conversion process to be self-sustaining [13]. These advantages have attracted considerable attention from scientists and engineers over the past decade making the analysis of SCWO processes in general, and hydrothermal flames in particular, of great interest. Apart from the technological relevance, hydrothermal flames provide a canonical system for studying combustion processes at very high pressures.

While a number of experimental studies of hydrothermal flames exist in the literature, there are only a few theoretical papers on the subject (e.g. [9,15] and references therein). In this paper, we formulate and analyse a simple model that provides a sharp characterization of autoignition in terms of the principal physical and geometric parameters. We hope that our results will be useful for guiding future studies of autoignition of laminar jets.

The paper is organized as follows. In §2, we derive a model of autoignition for laminar jets. In §3, we state the main results of the analysis of this model and provide heuristic arguments to give physical insight of these results as well as results of numerical simulations. Section 4 is dedicated to proof of the main results. In §5, we provide a summary of our results and a brief discussion of the direction of future research in this area.

2. Formulation of the model

A common experimental configuration for the studies of ignition and dynamics of hydrothermal flames consists of a combustion vessel and an injection inlet [16]. The vessel is filled with a fuel-rich mixture at supercritical conditions and a small amount of oxidizer in supercritical conditions is injected into the ambient at rest. Alternatively, a fuel-rich jet is injected into an oxidizing ambient, both being at a supercritical state. This process may lead to the ignition of an inverse diffusion or diffusion flame, respectively. Under certain hydrodynamic conditions, the jet of injected substance has approximately cylindrical shape with a circular cross section (figure 1). In such jets, the flow may be regarded as unidirectional with an axially uniform profile.

To model the process, we will make the following assumptions: the jet has a prescribed shape of a cylinder with circular cross section and fixed height; the velocity inside the jet is constant; an ignition, if successful, has to occur within the jet; the activation energy of the reaction is large; the chemical reaction occurs exclusively on the surface of the jet; prior to autoignition, both the fuel and the oxidizer are in excess on the surface of the jet; the heat exchange between the jet and the

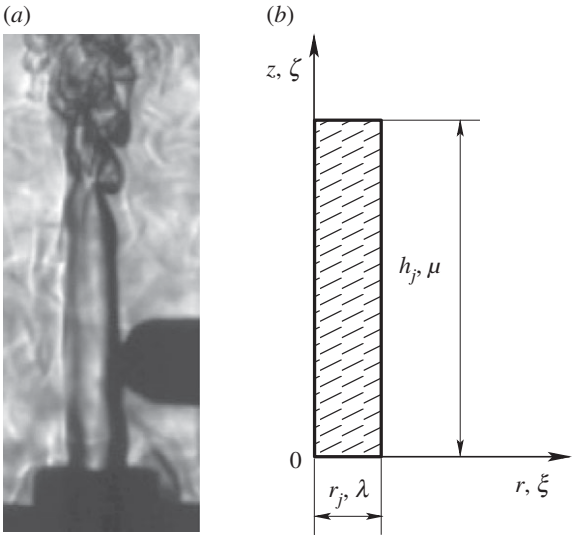

Figure 1. Jet injected into ambient at rest, both in supercritical state [16] (*a*) and its idealized approximation (*b*). The radius of the jet is approximately 1 mm and height is approximately 8 mm. The jet has a shape close to cylindrical.

ambient is negligible; diffusion in a vertical direction is negligible in comparison with advection; the temperature assumes a steady-state profile.

Under these assumptions, the equation governing the temperature field T inside the jet of radius r_j and height h_j is as follows:

$$c_p \rho u T_z = \kappa \left(T_{rr} + \frac{1}{r} T_r \right), \tag{2.1}$$

where κ is the thermal conductivity, u is the flow velocity within the jet, c_p and ρ are specific heat and density, r and z are coordinates in radial and vertical directions.

This equation should be complemented by a condition prescribing the jet temperature at the entrance to the vessel, namely

$$T = T_0 \quad \text{at } z = 0, \tag{2.2}$$

and the boundary condition on the surface of the jet

$$\kappa T_r = W(C_\mathrm{o}, C_\mathrm{f}, T) \quad \text{at } r = r_j. \tag{2.3}$$

The latter condition prescribes a flux of temperature on a jet surface due to the chemical reaction. The right-hand side of equation (2.3) is given by

$$W(C_\mathrm{o}, C_\mathrm{f}, T) = Q C_\mathrm{o}^0 C_\mathrm{f} \exp\left(-\frac{E}{RT} \right), \tag{2.4}$$

where Q is the reaction intensity, C_o and C_f are concentrations of the oxidizer and the fuel, E is the effective activation energy and R is the universal gas constant. Here C_o^0 means zero-order reaction with respect to oxygen [17].

Using the assumptions given above, we set the concentration of fuel and oxidizer on the surface of the jet to be equal to the initial concentrations ($C_\mathrm{f} = \bar{C}_\mathrm{f}, C_\mathrm{o} = \bar{C}_\mathrm{o}$). In addition, the assumption of high activation energy allows application of the Frank–Kamenetskii transform.

Therefore,

$$W(C_o, C_f, T) = QC_o^0 C_f \exp\left(-\frac{E}{RT}\right) \approx Q\bar{C}_f \exp\left(-\frac{E}{RT_0(1+(T-T_0)/T_0)}\right)$$
$$\approx Q\bar{C}_f \exp\left(-\frac{E}{RT_0}\right)\exp\left(\frac{E}{RT_0^2}(T-T_0)\right). \tag{2.5}$$

Introducing scaled temperature θ, scaled radius λ and height of the jet, μ, as well as the scaled radial ξ and vertical ζ coordinates

$$\left.\begin{aligned} \theta &= \frac{E}{RT_0^2}(T-T_0), \quad \lambda = \frac{Q\bar{C}_f}{k}\frac{E}{RT_0^2}\exp\left(-\frac{E}{RT_0}\right) r_j, \\ \mu &= \frac{Q^2\bar{C}_f^2}{kc_p\rho u}\left(\frac{E}{RT_0^2}\right)^2 \exp\left(-2\frac{E}{RT_0}\right) h_j, \\ \xi &= \frac{Q\bar{C}_f}{k}\frac{E}{RT_0^2}\exp\left(-\frac{E}{RT_0}\right) r \quad \text{and} \quad \zeta = \frac{Q^2\bar{C}_f^2}{kc_p\rho u}\left(\frac{E}{RT_0^2}\right)^2 \exp\left(-2\frac{E}{RT_0}\right) z, \end{aligned}\right\} \tag{2.6}$$

we obtain the following equation that governs the evolution of scaled temperature $\theta(\xi, \zeta)$ inside the jet:

$$\theta_\zeta = \theta_{\xi\xi} + \frac{1}{\xi}\theta_\xi, \quad \text{at } 0 < \xi < \lambda, \ \ 0 < \zeta < \mu, \tag{2.7}$$

supplemented by the initial-like condition

$$\theta = 0 \quad \text{at } \zeta = 0, \ \ 0 \le \xi \le \lambda, \tag{2.8}$$

and the boundary conditions,

$$\theta_\xi = \exp(\theta) \quad \text{at } \xi = \lambda, \ \ 0 < \zeta < \mu. \tag{2.9}$$

We also note that

$$\theta_\xi = 0 \quad \text{at } \xi = 0, \ \ 0 < \zeta < \mu \tag{2.10}$$

as required by symmetry.

A study of autoignition of the jet therefore reduces to the analysis of solutions of problem (2.7)–(2.9) that depend on two parameters: scaled radius of the jet λ and its scaled height μ. As we will show in §3, for fixed λ there exists $0 < \zeta^*(\lambda) < \infty$ such that solution of the problem (2.7)–(2.9) exists if $\mu < \zeta^*(\lambda)$ and blows up (becomes unbounded) as $\zeta \to \zeta^*$ when $\mu \ge \zeta^*$. In the framework of this theory, as in any theory based on the Frank–Kamenetskii approximation, autoignition is associated with thermal runaway, that is the 'blow up' of the solution of corresponding differential equations. Consequently, the autoignition condition reads

$$\zeta^*(\lambda) < \mu. \tag{2.11}$$

That is, autoignition (i.e. thermal runaway) has to occur within the jet.

It is important to note that problem (2.7)–(2.9) and autoignition condition (2.11) are quite different from classical models of autoignition [1,2]. The main difference of the model considered here is that the nonlinear reaction term appears in boundary condition (2.9), whereas in classical models the reaction term is present in the equation describing temperature field in the bulk. Models involving boundary reaction, however, were previously studied in the literature [4–6]. It is also worth mentioning that as the activation energy E is usually large, parameters λ and μ in problem (2.7)–(2.9) are very sensitive to even small variations in initial temperature T_0. Thus, the range of values for λ and μ may vary by orders of magnitude. Consequently, it is important to understand the qualitative behaviour of the ignition position $\zeta^*(\lambda)$ in the entire range of $\lambda \in (0, \infty)$.

In §3, we will give a full analysis of solutions for the problem and derive an approximate formula for the ignition position $\zeta^*(\lambda)$.

3. Analysis of the model

In this section, we will discuss properties of the solutions of problem (2.7)–(2.9). These properties are given by the following theorem.

Theorem 3.1. *For each $\lambda > 0$, there exists $0 < \zeta^*(\lambda) < \infty$ such that problem* (2.7)–(2.9) *has a unique classical solution $\theta(\xi, \zeta)$ provided $\mu < \zeta^*$.*

If $\mu \geq \zeta^*$, the solution of problem (2.7)–(2.9) *blows up as $\zeta \to \zeta^*$. The blow up position, ζ^*, is a bounded non-decreasing function of λ that obeys the following upper bound:*

$$\zeta^*(\lambda) \leq \min\left\{\frac{\lambda}{2}, \sigma_m\right\}, \tag{3.1}$$

where, $\sigma_m < 1$ is given by

$$\sigma_m = \sup\left\{\sigma > 0 | v(\sigma) = \frac{1}{\sqrt{\pi}} \int_0^\sigma \frac{\mathrm{e}^{v(s)}\,\mathrm{d}s}{\sqrt{\sigma - s}} \quad \textit{has a solution}\right\}. \tag{3.2}$$

Moreover, over the interval of its existence, the solution of problem (2.7)–(2.9) *is non-negative and non-decreasing in both ξ and ζ.*

Remark 3.2. Let us note that theorem 3.1 can be easily adopted for more general types of nonlinearities. In particular, for the case when the exponent on the right-hand side of equation (2.9) is replaced by a positive increasing convex C^1 function g satisfying $\int_0^\infty \mathrm{d}s/g(s) < \infty$.

A proof of theorem 3.1 is given in §4. Here, let us discuss the physical implications of theorem 3.1. The most important result of this theorem is that the autoignition position $\zeta^*(\lambda)$ is a bounded monotone function of its argument. The fact that $\zeta^*(\lambda)$ increases as λ increases is intuitively clear as a jet of larger radius can absorb more heat before ignition occurs. What is rather interesting is that even in the limit of infinite radius, the jet still ignites at a finite height. This means that with jets of substantial radius and height, which can absorb an extremely large amount of heat, the limiting factor is the heat transport from the surface of the jet to its interior. As is evident from our analysis, this heat transport is not sufficiently fast to prevent the autoignition of jets with height exceeding its critical value σ_m, regardless of the jet's radius.

Position of the autoignition point can be computed numerically and is presented on figure 2. This curve can be approximated with good accuracy by the following simple equation:

$$\zeta^*(\lambda) \approx \frac{\lambda}{2}\left(\frac{\mathrm{e}^\lambda}{1 + 0.5\lambda^2 + 1.8\lambda\,\mathrm{e}^\lambda}\right). \tag{3.3}$$

Let us now discuss the behaviour of this curve. One can see that for small values of λ, the ignition position $\zeta^*(\lambda)$ scales linearly with λ. This behaviour can be explained as follows. In the case when the radius of the jet is small enough, the temperature field is close to uniform in the entire jet, despite the fact that the reaction takes place only on the surface (figures 3 and 4). The substantial gradient of temperature is only seen for ζ close to ζ^*. Therefore, the average temperature of the cross section of the jet $\Theta(\zeta)$ is practically equal to the temperature on the boundary for ζ away from ζ^*. As a result, upon integration of (2.7) and taking into account boundary conditions (2.9), we have (see step 5 of theorem 3.1 for more details)

$$\frac{\mathrm{d}\Theta}{\mathrm{d}\zeta} \approx \frac{2}{\lambda}\exp(\Theta). \tag{3.4}$$

As $\Theta(0) = 0$, we obtain from (3.4)

$$\Theta(\zeta) \approx -\ln\left(1 - \frac{2\zeta}{\lambda}\right) \tag{3.5}$$

which in turn gives

$$\zeta^*(\lambda) \approx \frac{\lambda}{2}, \quad \lambda \ll 1. \tag{3.6}$$

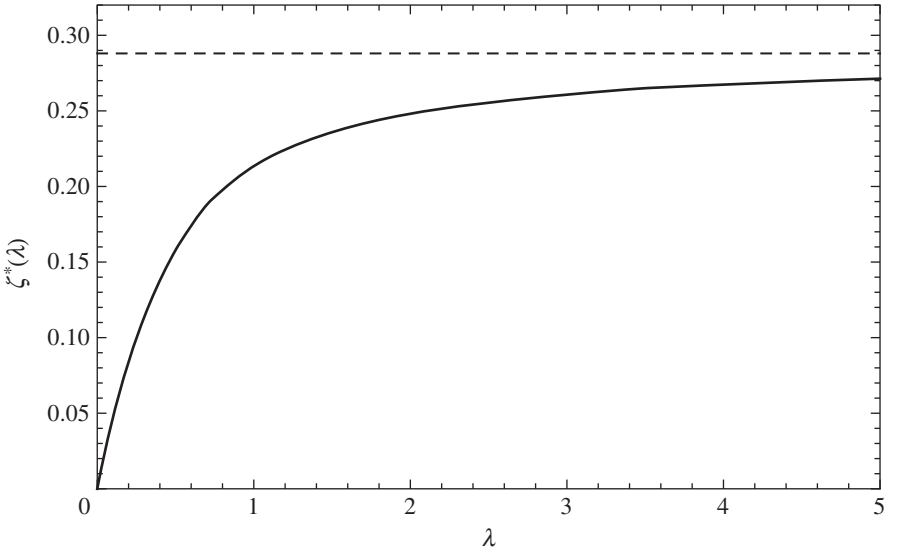

Figure 2. Scaled height of ignition versus scaled radius of the jet (solid line). The height of the jet increases as radius increases. For small jet radius, the height scales almost linearly with radius and saturates to a limiting value (dashed line) when radius increases. The dependency of ignition height on radius of the jet completely agrees with conclusions of theorem 3.1.

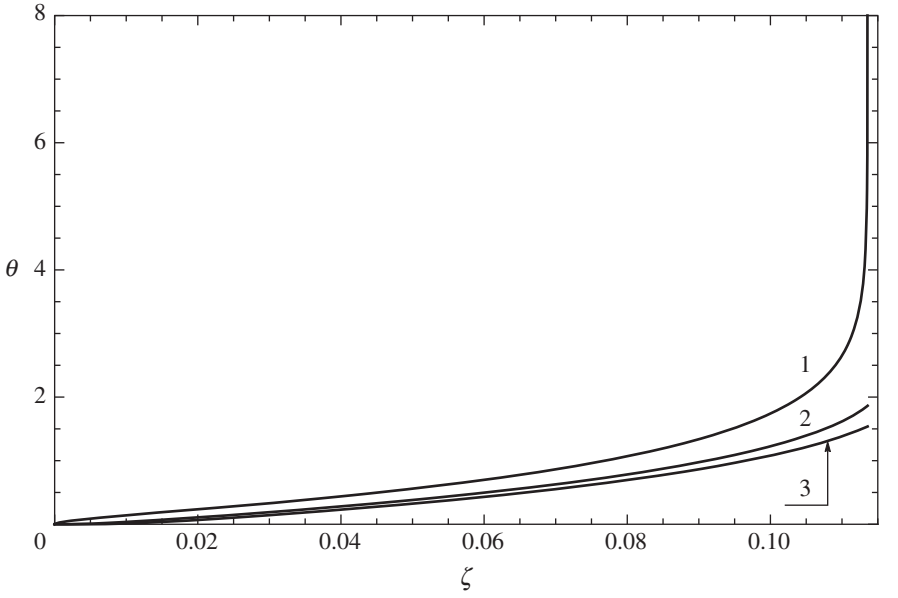

Figure 3. Temperature distribution as a function of ζ on a surface of the jet (1), at half of its radius (2) and in the middle of the jet (3), respectively, with scaled radius of the jet $\lambda = 0.3$.

One can see from figure 2 that the function $\zeta^*(\lambda)$ is reasonably close to a linear function for $\lambda \leq 0.5$, and thus (3.6) is applicable in this range of λ. Let us also note that equation (3.4) is formally identical to a classical Semenov model of thermal explosion in the absence of heat loss [2].

As the radius of the jet increases, the curve $\zeta^*(\lambda)$ starts to deviate substantially from the linear function. This is due to the fact that when λ increases, a sharp boundary layer starts to form near

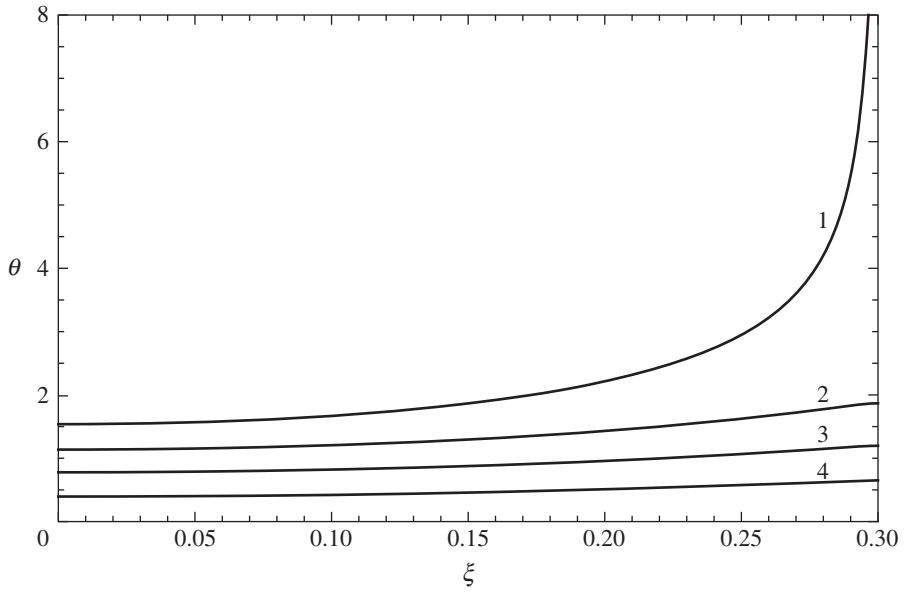

Figure 4. Temperature distribution over the cross section of the jet at $\zeta = 0.5\zeta^*(4)$, $\zeta = 0.75\zeta^*(3)$, $\zeta = 0.9\zeta^*(2)$ and $\zeta \approx \zeta^*(1)$, respectively, with the scaled radius of the jet $\lambda = 0.3$. Temperature field is close to uniform over the cross sections of the jet, except the vicinity of the ignition point.

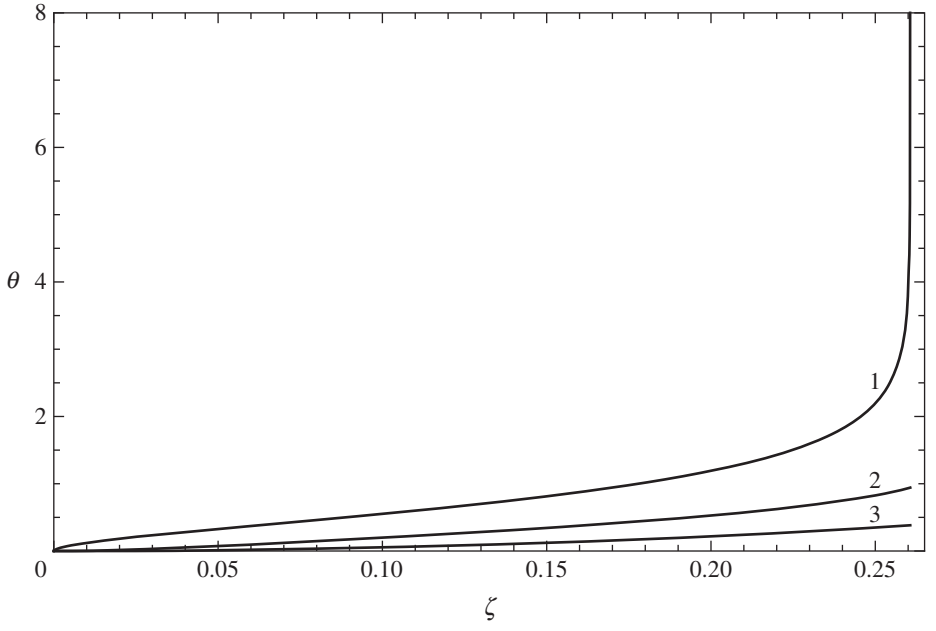

Figure 5. Temperature distribution as a function of ζ on the surface of the jet (1), at 90% (2) and 80% (3) of its radius, respectively, with scaled radius of the jet $\lambda = 3$. One can see a significant drop in the temperature inside the jet in comparison to its surface temperature.

the surface of the jet. Consequently, the average temperature of the jet's cross section becomes substantially smaller than its maximal value attained at the jet's surface (figures 5 and 6). For large enough λ, the temperature is essentially zero except for some small (order of unity) vicinity of the jet's surface. As a result, when λ is sufficiently large, the solution of problem (2.7)–(2.9)

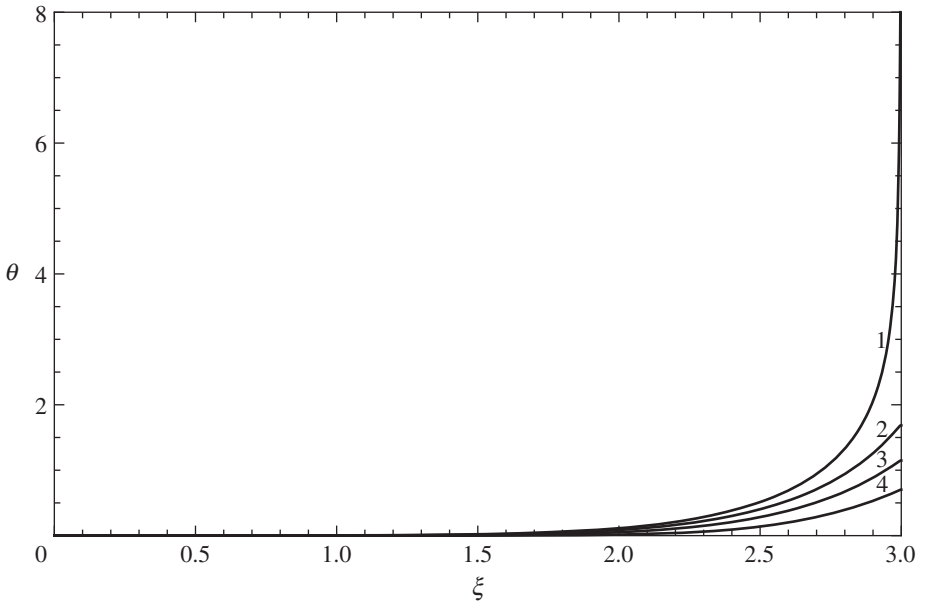

Figure 6. Temperature distribution over the cross section of the jet at $\zeta = 0.5\zeta^*$ (4), $\zeta = 0.75\zeta^*$ (3), $\zeta = 0.9\zeta^*$ (2) and $\zeta \approx \zeta^*$(1), respectively, with scaled radius of the jet $\lambda = 3$. The temperature field forms a boundary layer near surface of the jet and essentially zero near its middle.

becomes indistinguishable from the solution of the one-dimensional heat equation posed on the half line. That is, the solution of the following boundary value problem:

$$\left.\begin{aligned} \vartheta_\zeta &= \vartheta_{\xi\xi} && \xi > 0, \quad 0 < \zeta < \mu, \\ \vartheta_\xi &= \exp(\vartheta) && \xi = 0, \quad 0 < \zeta < \mu \\ \vartheta &= 0 && \xi > 0, \quad \zeta = 0. \end{aligned}\right\} \tag{3.7}$$

and

One can show using simple reflection arguments that the solution of this problem, evaluated at the boundary $v(\zeta) = \vartheta(0, \zeta)$, solves the following integral equation:

$$v(\zeta) = \frac{1}{\sqrt{\pi}} \int_0^\zeta \exp(v(\zeta')) \frac{\mathrm{d}\zeta'}{\sqrt{\zeta - \zeta'}}. \tag{3.8}$$

The equation has a solution for $\zeta < \sigma_m$ and blows up as $\zeta \to \sigma_m$. The value of $\sigma_m \approx 0.28$ was estimated numerically and as a result, for sufficiently large values of λ, we have

$$\zeta^*(\lambda) \approx 0.28, \quad \lambda \gg 1. \tag{3.9}$$

One can see from figure 2 that equation (3.9) is a good approximation of $\zeta^*(\lambda)$ for $\lambda > 3$.

In the following section, we give a proof of theorem 3.1.

4. Proof of theorem 3.1

In this section, we give a proof of the main theorem stated in the previous section. Part of the proof of the theorem is based on a simple version of the classical parabolic comparison principle [18–20] which is given by the following proposition.

Proposition 4.1 (Parabolic comparison principle). *Let*

$$\left.\begin{aligned} P[w] &= w_\zeta - w_{\xi\xi} - \frac{1}{\xi} w_\xi - \alpha \\ \text{and} \qquad Q[w] &= w_\xi - \beta, \end{aligned}\right\} \tag{4.1}$$

where $\alpha = \alpha(\xi, \zeta)$ and $\beta = \beta(\xi, \zeta, w)$ are some given functions.

Assume that there exist continuous bounded functions $\underline{w}$ and $\bar{w}$ with continuous first derivatives in ζ and continuous first and second derivatives in ξ that satisfy differential inequalities

$$\left.\begin{aligned} P[\underline{w}] &\le 0 \quad 0 < \xi < \lambda \quad 0 < \zeta < \mu, \\ Q[\underline{w}] &\le 0 \quad \xi = \lambda \quad 0 < \zeta < \mu \\ \text{and} \qquad \underline{w} &\le w_0 \quad 0 \le \xi \le \lambda \quad \zeta = 0, \end{aligned}\right\} \tag{4.2}$$

and

$$\left.\begin{aligned} P[\bar{w}] &\ge 0 \quad 0 < \xi < \lambda \quad 0 < \zeta < \mu, \\ Q[\bar{w}] &\ge 0 \quad \xi = \lambda \quad 0 < \zeta < \mu \\ \bar{w} &\ge w_0 \quad 0 \le \xi \le \lambda \quad \zeta = 0, \end{aligned}\right\} \tag{4.3}$$

respectively, where w_0 is a given function.

Then,

$$\underline{w}(\xi, \zeta) \le \bar{w}(\xi, \zeta) \quad 0 \le \xi \le \lambda, \quad 0 \le \zeta < \mu. \tag{4.4}$$

Existence of functions $\underline{w}$ and $\bar{w}$ with properties described above imply the existence of the classical solution for the following initial boundary value problem:

$$\left.\begin{aligned} P[w] &= 0 \quad 0 < \xi < \lambda \quad 0 < \zeta < \mu, \\ Q[w] &= 0 \quad \xi = \lambda \quad 0 < \zeta < \mu \\ \text{and} \qquad w &= w_0 \quad 0 \le \xi \le \lambda \quad \zeta = 0 \end{aligned}\right\} \tag{4.5}$$

that satisfies

$$\underline{w}(\xi, \zeta) \le w(\xi, \zeta) \le \bar{w}(\xi, \zeta) \quad 0 \le \xi \le \lambda, \quad 0 \le \zeta < \mu \tag{4.6}$$

and functions $\underline{w}$ and $\bar{w}$ are called sub- and super-solutions of problem (4.5).

Now we turn to the proof of theorem 3.1.

Proof of theorem 3.1. The proof proceeds in several steps.

Step 1. Short time existence and uniqueness and finite height blow up.

Existence of a unique classical solution for problem (2.7)–(2.9) with μ sufficiently small, as well as the fact that the solution of this problem blows up provided μ is large enough, were established in [21] (see also [22] for a more general framework).

Step 2. Non-negativity and monotonicity of solution.

Let us now show that on the entire interval of its existence, the solution of problem (2.7)–(2.9) satisfies $\theta, \theta_\zeta, \theta_\xi \ge 0$.

Assume that the classical solution of problem (2.7)–(2.9) exists for $\zeta \in [0, \mu_1)$ for some $\mu_1 > 0$. The fact that $\theta \ge 0$ is a direct consequence of parabolic comparison principle, as $\theta = 0$ is a sub-solution for problem (2.7)–(2.9). We now turn to the monotonicity properties of θ. We start with the monotonicity in ζ. Let $\psi(\xi, \zeta) = \theta(\xi, \zeta + \tau)$. As $\psi(\xi, 0) = \theta(\xi, \tau) \ge 0$, we have by the comparison principle $w(\xi, \zeta) \ge \theta(\xi, \zeta)$ for $\xi \in [0, \lambda]$, $\zeta \in (0, \mu_1 - \tau)$. Thus, for any $\tau > 0$, we have $(\psi(\xi, \zeta) - \theta(\xi, \zeta))/\tau \ge 0$. Taking the limit as $\tau \to 0$, we have $\theta_\zeta \ge 0$. To show the monotonicity in ξ, we integrate equation (2.7) with respect to ξ that gives

$$\theta_\xi(\xi, \zeta) = \frac{1}{\xi} \int_0^\xi \theta_\zeta(\xi', \zeta) \xi' \, \mathrm{d}\xi'. \tag{4.7}$$

Taking into account that $\theta_\zeta \ge 0$, we have $\theta_\xi \ge 0$.

Step 3. Monotonicity of blow up position ζ^* in λ.

Now let us show that $\zeta^*(\lambda)$ is a non-decreasing function of its argument. Let $\lambda_2 > \lambda_1$ and set $\phi_1(\xi,\zeta) := \theta_{\lambda_1}(\xi,\zeta)$ and $\phi_2(\xi,\zeta) := \theta_{\lambda_2}(\xi+\lambda_2-\lambda_1,\zeta)$, $\eta(\xi,\zeta) := \phi_1(\xi,\zeta) - \phi_2(\xi,\zeta)$. Assume that both solutions θ_{λ_1} and θ_{λ_2} are classical for $\zeta \in [0,\mu_2)$ for some $\mu_2 > 0$. It then follows from equation (2.7) that

$$\eta_\zeta = \eta_{\xi\xi} + \frac{1}{\xi}\eta + \frac{\lambda_2-\lambda_1}{\xi(\lambda_2-\lambda_1+\xi)}(\phi_2)_\xi, \quad 0<\xi<\lambda_1, \quad 0<\zeta<\mu_2. \tag{4.8}$$

Moreover, from equations (2.8) and (2.9), we have

$$\eta_\xi(\lambda_1,\zeta) = \exp(\phi_1(\lambda_1,\zeta)) - \exp(\phi_2(\lambda_2,\zeta) = \exp(\tilde{\phi})\eta(\lambda_1,\zeta) \quad 0<\zeta<\mu_2, \tag{4.9}$$

where $\tilde{\phi}$ is some function between ϕ_1 and ϕ_2, and

$$\eta(\xi,0) = 0, \quad 0 \le \xi \le \lambda_1. \tag{4.10}$$

In a view of the fact that $(\phi_2)_\xi \ge 0$, we conclude that $\eta = 0$ is a sub-solution for problem (4.8)–(4.10) and thus $\phi_1(\xi,\zeta) \ge \phi_2(\xi,\zeta)$ for all $\xi \in [0,\lambda]$ and $\zeta \in [0,\mu_2)$. By monotonicity of solutions of problem (2.7)–(2.9) established in Step 2 of this theorem, we have

$$\sup_{\xi\in[0,\lambda_1],\zeta\in[0,\mu_2)} \theta_{\lambda_1}(\xi,\zeta) \ge \sup_{\xi\in[0,\lambda_2],\zeta\in[0,\mu_2)} \theta_{\lambda_2}(\xi,\zeta) \tag{4.11}$$

and therefore θ_{λ_2} cannot blow up before θ_{λ_1}.

Step 4. Limiting behaviour of solution as $\lambda \to \infty$.

Observe first that since θ solves the heat equation (2.7) in a disc of radius λ, we can represent the solution of this equation on a boundary of this disc in an integral form

$$\theta(\lambda,\zeta) = 2\int_0^\zeta \int_{\partial B_\lambda} \left\{ K(\mathbf{r}-\mathbf{r}',\zeta-\zeta')\frac{\partial}{\partial\nu}\theta(\lambda,\zeta') - \frac{\partial}{\partial\nu_{\mathbf{r}'}}K(\mathbf{r}-\mathbf{r}',\zeta-\zeta')\theta(\lambda,\zeta') \right\} \mathrm{d}S(\mathbf{r}')\,\mathrm{d}\zeta', \tag{4.12}$$

where ∂B_λ and $\mathrm{d}S(\mathbf{r}')$ are circle and element of length of a circle of radius λ, $\mathbf{r}$ and $\mathbf{r}'$ are position vectors of an arbitrary fixed and arbitrary point on a circle of radius λ, ν is an outward unit normal to a circle and

$$K(\mathbf{r},\zeta) = \frac{1}{4\pi\zeta}\exp\left(-\frac{|\mathbf{r}|^2}{4\zeta}\right) \tag{4.13}$$

is a heat kernel.

Equation (4.12) follows from the standard representation formula for the solution of a heat equation [23, ch. 4] and the jump condition on the normal derivative of the heat kernel [23, lemma 4.3.2]. After straightforward computations, we obtain, from equation (4.12) with boundary condition (2.9), the following integral equation:

$$\theta(\lambda,\zeta) = \frac{1}{\sqrt{\pi}}\int_0^\zeta R_1\left(\frac{\lambda}{\sqrt{\zeta-\zeta'}}\right)\exp(\theta(\lambda,\zeta')\frac{\mathrm{d}\zeta'}{\sqrt{\zeta-\zeta'}} - \int_0^\zeta R_0\left(\frac{\lambda}{\sqrt{\zeta-\zeta'}}\right)\theta(\lambda,\zeta')\,\mathrm{d}\zeta', \tag{4.14}$$

where

$$R_0(s) = 4s^2\,\mathrm{e}^{-s^2}(I_0(s^2) - I_1(s^2)) \quad \text{and} \quad R_1(s) = \sqrt{2\pi}s\,\mathrm{e}^{-s^2}I_0(s^2). \tag{4.15}$$

Here, I_n are modified Bessel functions of the first kind [24]. One can verify that

$$R_0(s) \to 0, \quad R_1(s) \to 1 \quad \text{as } s \to \infty. \tag{4.16}$$

Therefore, for any fixed interval of ζ where the classical solution of problem (2.7)–(2.9) exists, we have $\theta(\lambda,\zeta) \to v(\zeta)$ as $\lambda \to \infty$, where $v(\zeta)$ solves an integral equation

$$v(\zeta) = \frac{1}{\sqrt{\pi}}\int_0^\zeta \exp(v(\zeta'))\frac{\mathrm{d}\zeta'}{\sqrt{\zeta-\zeta'}}. \tag{4.17}$$

As we mentioned in §3, equation (4.17) gives solution of problem (3.7) evaluated at the boundary, which then gives the behaviour when $\lambda \to \infty$.

Step 5. Upper bound on the blow up position.

Let us first give a global upper bound on $\zeta^*(\lambda)$. As follows from the result of the previous step, as $\lambda \to \infty$, the solution of problem (2.7)–(2.9) evaluated at the boundary of the jet obeys the integral equation (4.17). By the classical inversion formula (e.g. [25]), we then have

$$\exp(v(\zeta)) = \frac{1}{\sqrt{\pi}} \frac{\mathrm{d}}{\mathrm{d}\zeta} \int_0^\zeta v(\zeta) \frac{\mathrm{d}\zeta'}{\sqrt{\zeta - \zeta'}}. \tag{4.18}$$

Combining equations (4.17) and (4.18), we have

$$\frac{1}{\sqrt{\pi}} \frac{\mathrm{d}}{\mathrm{d}\zeta} \left(\int_0^\zeta v(\zeta) \frac{\mathrm{d}\zeta'}{\sqrt{\zeta - \zeta'}} \right) = \exp\left(\frac{1}{\sqrt{\pi}} \int_0^\zeta \exp(v(\zeta')) \frac{\mathrm{d}\zeta'}{\sqrt{\zeta - \zeta'}} \right). \tag{4.19}$$

Setting

$$g(\zeta) = \frac{1}{\sqrt{\pi}} \int_0^\zeta v(\zeta) \frac{\mathrm{d}\zeta'}{\sqrt{\zeta - \zeta'}} \tag{4.20}$$

and observing that

$$\frac{1}{\sqrt{\pi}} \int_0^\zeta \exp(v(\zeta')) \frac{\mathrm{d}\zeta'}{\sqrt{\zeta - \zeta'}} > g(\zeta), \tag{4.21}$$

we have

$$\frac{\mathrm{d}}{\mathrm{d}\zeta} g(\zeta) > \exp(g(\zeta)). \tag{4.22}$$

As $g(0) = 0$, we conclude

$$g(\zeta) > -\ln(1 - \zeta) \tag{4.23}$$

and thus $g(\zeta)$ and therefore $v(\zeta)$ blows up at a point $\zeta^* < 1$. As $\zeta^*(\lambda)$ is a non-decreasing function in λ, we conclude that $\zeta^* < 1$ is a global upper bound for all λ.

Let us show that the solution of problem (2.7)–(2.9) blows up at the position $\zeta^*(\lambda) \le \lambda/2$. Integrating equation (2.7) in ξ and taking into account boundary condition (2.9), we have

$$\frac{\mathrm{d}\Theta(\zeta)}{\mathrm{d}\zeta} = \frac{2}{\lambda} \exp(\theta(\lambda, \zeta)), \tag{4.24}$$

where

$$\Theta(\zeta) = \frac{2}{\lambda} \int_0^\lambda \theta(\xi, \zeta) \xi \, \mathrm{d}\xi \tag{4.25}$$

is an average value of temperature θ over a circular cross section of the jet. By maximum principle and monotonicity of θ in both variables, we have that $\max_{\xi \in [0,\lambda], \zeta \in [0,\bar{\zeta}]} \theta(\xi, \zeta) = \theta(\lambda, \bar{\zeta})$. In particular, it implies that $\theta(\lambda, \zeta) \ge \Theta(\zeta)$, which in combination with (3.2) gives

$$\frac{\mathrm{d}\Theta(\zeta)}{\mathrm{d}\zeta} \ge \frac{2}{\lambda} \exp(\Theta(\zeta)). \tag{4.26}$$

Since by equation (2.8) $\Theta(0) = 0$, we have from equation (4.26) that

$$\Theta(\zeta) \ge -\ln\left(1 - \frac{2}{\lambda}\zeta\right). \tag{4.27}$$

Thus, an average value of temperature blows up at $\zeta \le \lambda/2$, and in a view of non-negativity and monotonicity of θ, we then have $\zeta^*(\lambda) \le \lambda/2$. After combining the results of this step, we then have equation (3.1). ■

Remark 4.2. It follows directly from the proof of theorem 3.1 that analysis of problem (2.7)–(2.9) in the limiting cases of small and large λ reduces to analysis of the following equation:

$$\frac{\mathrm{d}^\alpha v}{\mathrm{d}s^\alpha} = \exp(v), \tag{4.28}$$

where v is temperature on the surface of the jet, s is a scaled coordinate along the jet, $\alpha = 1$, $s = 2\zeta/\lambda$ in the limit of small λ and $\alpha = \frac{1}{2}$, $s = \zeta$ in the limit of large λ. This, in particular, implies that near

the blow up position (height of ignition) s^* the temperature of the surface of the jet asymptotically behaves as follows:

$$v(s) \approx -\alpha \log(s^* - s). \tag{4.29}$$

5. Concluding remarks

In this paper, we have developed and fully analysed a simple model for autoignition of a laminar jet injected into ambient at rest. The motivation for this study was a renewed interest in hydrothermal flames in the SCWO environment. As a result of our analysis, we have derived a sharp condition for autoignition of such flames. With a good accuracy, this condition in dimensional form reads

$$\frac{\mathrm{e}^{\lambda}}{1+0.5\lambda^2+1.8\lambda\,\mathrm{e}^{\lambda}} < 2\frac{Q\bar{C}_{\mathrm{f}}}{c_p\rho u}\frac{E}{RT_0^2}\exp\left(-\frac{E}{RT_0}\right)\frac{h_j}{r_j}, \quad \lambda = \frac{Q\bar{C}_{\mathrm{f}}}{k}\frac{E}{RT_0^2}\exp\left(-\frac{E}{RT_0}\right)r_j, \tag{5.1}$$

where all physical and geometrical parameters are given in §2.

Equation (5.1) connects the principal physical and geometric parameters of the problem considered in this paper, showing that the autoignition occurs when the height of the jet is sufficiently large. Additionally, our results show that the temperature of the jet increases from the inlet position to an ignition point along the axial length of the flow. Given sufficient energy release from the ignition kernel a stable flame will develop and then become elevated from the inlet point. These observations are in qualitative agreement with experimental observations of ignition and oxidation in a supercritical environment [14,26,27]. Equation (5.1) may be used for assessing appropriate experimental parameters (e.g. flow rates, bulk fluid temperature and reactant concentrations) in future experimental work on hydrothermal flames. Additionally, this work provides a first step in understanding the linkages between the dominant fundamental physical processes upon which more complicated first-order analytical models will be developed. Future work will use a similar modelling approach to develop a flame ignition model using a co-flow burner configuration.

Data accessibility. The paper is theoretical and contains no data.

Authors' contributions. P.V.G., D.J.G, U.G.H., M.C.H., M.J.K. and G.I.S. formulated the model and analysed the results. P.V.G., M.C.H. and G.I.S. drafted the manuscript. P.V.G. performed mathematical and numerical analysis of the model. All authors gave final approval for publication.

Competing interests. We have no competing interests.

Funding. The work of D.J.G, U.G.H., M.C.H. and M.J.K. was supported by the NASA Space Life and Physical Sciences Research and Applications Program. The work of P.V.G. and G.I.S. was supported, in part, by the US-Israel Binational Science Foundation under grant no. 2012057. G.I.S. also acknowledges support of the Israel Science Foundation via grant no. 335/13. P.V.G. was also supported by grant no. 317882 from Simons Foundation.

Acknowledgements. Part of this work was done when P.V.G. was visiting NASA Glenn Research Center under the NASA Glenn Faculty Fellowship Program (NGFFP 2014). He thanks the Combustion Physics and Reacting Processes Branch of NASA Glenn Research Center for their hospitality. P.V.G. also thanks V. Moroz and C.B. Muratov for very valuable discussions and J. Coleman for creating excellent work environment.

References

1. Frank-Kamenetskii DA. 1969 *Diffusion and heat transfer in chemical kinetics*. New York, NY: Plenum Press.
2. Zeldovich Ya B, Barenblatt GI, Librovich VB, Makhviladze GM. 1985 *The mathematical theory of combustion and explosions*. New York, NY: Consultants Bureau [Plenum].
3. Barenblatt GI, Chorin AJ, Kast A. 1997 The influence of the flow of the reacting gas on the conditions for a thermal explosion. *Proc. Natl Acad. Sci. USA* **94**, 12 762–12 764. (doi:10.1073/pnas.94.24.12762)
4. Im HG, Bechtold JK, Law CK. 1993 Analysis of thermal ignition in supersonic flat-plate boundary layers. *J. Fluid Mech.* **249**, 99–120. (doi:10.1017/S0022112093001090)

5. Linan A, Williams FA. 1971 Theory of ignition of reactive solids by constant energy flux. *Combust. Sci. Technol.* **3**, 91–98. (doi:10.1080/00102207108952276)
6. Grosch CE, Jackson TL. 1991 Ignition and structure of laminar diffusion flame in a compressible mixing layer with finite rate chemistry. *Phys. Fluids A* **3**, 3087–3097. (doi:10.1063/1.857853)
7. Gordon PV, Moroz V. 2014 Gelfand-type problem for two-phase porous media. *Proc. R. Soc. A* **470**, 20130573. (doi:10.1098/rspa.2013.0573)
8. Linan A. 1974 The asymptotic structure of counterflow diffusion flames for large activation energies. *Acta Astronaut.* **1**, 1007–1039. (doi:10.1016/0094-5765(74)90066-6)
9. Fong D, Bechtold JK, Law CK. 2012 Asymptotic structure of laminar diffusion flames at high pressure. *Phys. Fluids* **24**, 093602. (doi:10.1063/1.4748344)
10. Linan A, Vera M, Sanchez AL. 2015 Ignition, litfoff, and extinction of gaseous diffusion flames. *Annu. Rev. Fluid Mech.* **47**, 293–314. (doi:10.1146/annurev-fluid-010814-014711)
11. Schilling W, Franck EU. 1988 Combustion and diffusion flames at high pressures to 2000 bar. *Ber. Bunsen-Ges. Phys. Chem. Chem. Phys.* **92**, 631–636. (doi:10.1002/bbpc.198800149)
12. Augustine C, Tester J. 2009 Hydrothermal flames: from phenomenological experimental demonstrations to quantitative understanding. *J. Supercritical Fluids* **47**, 415–430. (doi:10.1016/j.supflu.2008.10.003)
13. Prikopsky K, Wellig B, von Rohr R. 2007 SCWO of salt containing artificial wastewater using transpiring-wall reactor: experimental results. *J. Supercritical Fluids* **40**, 246–257. (doi:10.1016/j.supflu.2006.05.007)
14. Serikawa R, Usui T, Nishimura T, Hirokazu S, Shusaku H, Hideo S. 2002 Hydrothermal flames in supercritical water oxidation: investigation in a pilot scale continuous reactor. *Fuel* **81**, 1147–1159. (doi:10.1016/S0016-2361(02)00015-7)
15. Margolis SB, Johnston SC. 1989 Multiplicity and stability of supercritical combustion in a non-adiabatic tubular reactor. *Combust. Sci. Technol.* **65**, 103–136. (doi:10.1080/00102208908924044)
16. Hegde U, Gotti D, Hicks M. 2014 The transition to turbulence of buoyant near-critical water jets. *J. Supercritical Fluids* **95**, 195–203. (doi:10.1016/j.supflu.2014.08.005)
17. Halgate HR, Tester JW. 1993 Fundamental kinetics and mechanism of hydrogen oxidation in supercritical water. *Combust. Sci. Technol.* **88**, 369–397. (doi:10.1080/00102209308947245)
18. Friedman A. 1964 *Partial differential equations of parabolic type*. Englewood Cliffs, NJ: Prentice-Hall, Inc.
19. Walter W. 2002 Nonlinear parabolic differential equations and inequalities. *Discrete Contin. Dyn. Syst.* **8**, 451–468. (doi:10.3934/dcds.2002.8.451)
20. Pucci P, Serrin J 2007 *The maximum principle*. Progress in Nonlinear Differential Equations and their Applications, vol. 73. Basel, Switzerland: Birkhauser Verlag.
21. Walter W. 1975 On existence and nonexistence in the large of solutions of parabolic differential equations with a nonlinear boundary condition. *SIAM J. Math. Anal.* **6**, 85–90. (doi:10.1137/0506008)
22. Taylor ME 2011 *Partial differential equations III. Nonlinear equations*, 2nd edn. Applied Mathematical Sciences, vol. 117. New York, NY: Springer.
23. Jost J 2007 *Partial differential equations*, 2nd edn. Graduate Texts in Mathematics, vol. 214. New York, NY: Springer.
24. Abramowitz M, Stegun IA. 1964 *Handbook of mathematical functions with formulas, graphs, and mathematical tables*. Washington, DC: U.S. Government Printing Office.
25. Tamarkin JD. 1930 On integrable solutions of Abel's integral equation. *Ann. Math.* **31**, 219–229. (doi:10.2307/1968092)
26. Hicks M, Lauver R, Hegde U, Sikora T. 2006 Diffusion limited Supercritical Water Oxidation (SCWO) in microgravity environments. SAE Technical Paper 2006-01-2132.
27. Steeper RR, Rice SF, Brown MS, Johnston SC. 1992 Methane and methanol diffusion flames in supercritical water. *J. Supercritical Fluids* **5**, 262–268. (doi:10.1016/0896-8446(92)90017-E)